A 37–43 GHz Endfire Antenna Element Based on Ball Grid Array Packaging for 5G Wireless Systems

Xiubo Liu[1], Wei Zhang[1], Dongning Hao[1], and Yanyan Liu[2, *]

Abstract—A 37–43 GHz endfire antenna based on ball grid array (BGA) packaging is proposed for the fifth-generation (5G) wireless system. The antenna consists of a miniaturized radiator and reflector. Besides, the radiator is fed by a substrate integrated waveguide (SIW). Furthermore, the RF transition from the SIW to grounded coplanar waveguide (GCPW) and vertical quasi-coaxial is realized on the substrate. The antenna is implemented on a single-layer substrate using standard printed circuit board (PCB) technology to reduce costs. Then, the cost-effective antenna element is reflow soldered with solder balls to form a BGA packaging. The advantages of the BGA packaging and the three-dimensional (3D) integration are discussed in detail. The miniature packaging achieves a compact size of $7 \, \text{mm} \times 3.4 \, \text{mm} \times 0.6 \, \text{mm}$. Finally, a prototype was manufactured to verify the performance. The measurement results show that the proposed antenna is a good candidate for 5G millimeter-wave (mmWave) New Radio (NR) applications.

1. INTRODUCTION

Nowadays, 5G expands the spectrum to higher frequencies and obtains sufficient bandwidth for the ever-increasing demand for communication. Emerging 5G systems require highly integrated functions to achieve high data rates, low power consumption, and high efficiency [1, 2]. Extensive research has been carried out on 5G millimeter-wave antennas, for example, Huygens source antenna [3], omnidirectional circularly polarized antenna [4], and titled combined beam antenna [5]. However, the above-mentioned antennas must be interconnected with the RF chipset using lossy waveguide connectors or coaxial connectors. Most importantly, the connector is too bulky to be integrated into the RF system.

Antenna-in-Package (AiP) is a key technology that integrates antenna and RF front-end chipsets in the same package to obtain higher performance for the 5G wireless system [6–8]. AiP technology can integrate antenna and RF chip into the same package. The main point is that it reduces the insertion loss between the RF chip and the antenna, thereby improving the performance of the system. The AiP can be achieved by glass-based packaging [9], silicon-based packaging [10], and LTCC-based packaging [11, 12]. Nevertheless, compared with organic laminates [15, 16], their manufacturing costs are higher. The antennas made on the printed circuit board (PCB) have better performance and cost advantage. In particular, the antenna on a single-layer substrate will greatly reduce the cost.

Recently, the stacked 3D packaging can integrate RF, analog, digital, power management chipsets, passive devices, and antenna in one package while maintaining miniaturization. Besides, the component density of 3D packaging is higher than that of 2D packages, which reduces the feed-line loss between the devices and improves the system performance [8, 16, 17]. Most importantly, the integrated antenna overcomes the shortcomings of discrete antennas that are difficult to integrate into the system using connector interconnections. Flip-chip interconnection technology replaces the wire bonding, resulting in

lower parasitic effects and better RF performance. Furthermore, the flip-chip interconnections are based on mature surface-mount technology (SMT) to reduce costs. Packaged antennas can be divided into three categories, which are BGA packaging [18–20], QFN packaging [13, 14], and eWLB packaging [21]. Among them, the BGA package and eWLB packaging are based on small solder balls, bumps, or pillars, so they can effectively reduce parasitic effects and operate at high frequencies.

In this letter, we proposed a BGA packaged endfire antenna element for the 5G mmWave wireless system. Only a single dielectric layer is used to achieve cost-effective features. In addition, the introduction of BGA packaging reduces the size of the antenna. In addition, the standard BGA package is suitable for automatic assembly, thereby improving production efficiency. Therefore, the proposed surface mount antenna element based on the BGA package is suitable for 5G millimeter-wave system integration. The antenna design and verification are described in detail in the following section. All simulation results are given by Ansys HFSS.

2. ANTENNA DESIGN

2.1. Antenna Geometry

Figure 1 shows the geometry of the proposed antenna. The exploded view, top view, and bottom view are shown in detail, respectively. The antenna is made on the Rogers4350B with a dielectric constant of 3.66, a dielectric loss tangent of 0.004, and a thickness of 0.254 mm. Besides, the antenna consists of two mirrored bowtie patches located on both sides of the substrate. The bottom metal can be regarded as a reflector that directs the beam. The substrate integrated waveguide excites the bowtie patches with the same amplitude and differential phase. Plated through-hole with a diameter of 0.2 mm connects the top metal and bottom metal. Solder resist is made on the bottom layer and is used to fix the solder balls during the reflow soldering process. Finally, the solder balls with a diameter of 300 μm are mounted on the bottom layer. The detailed dimensions of the prototype are listed in Table 1. Finally, the antenna size is 7 mm × 3.4 mm × 0.6 mm.
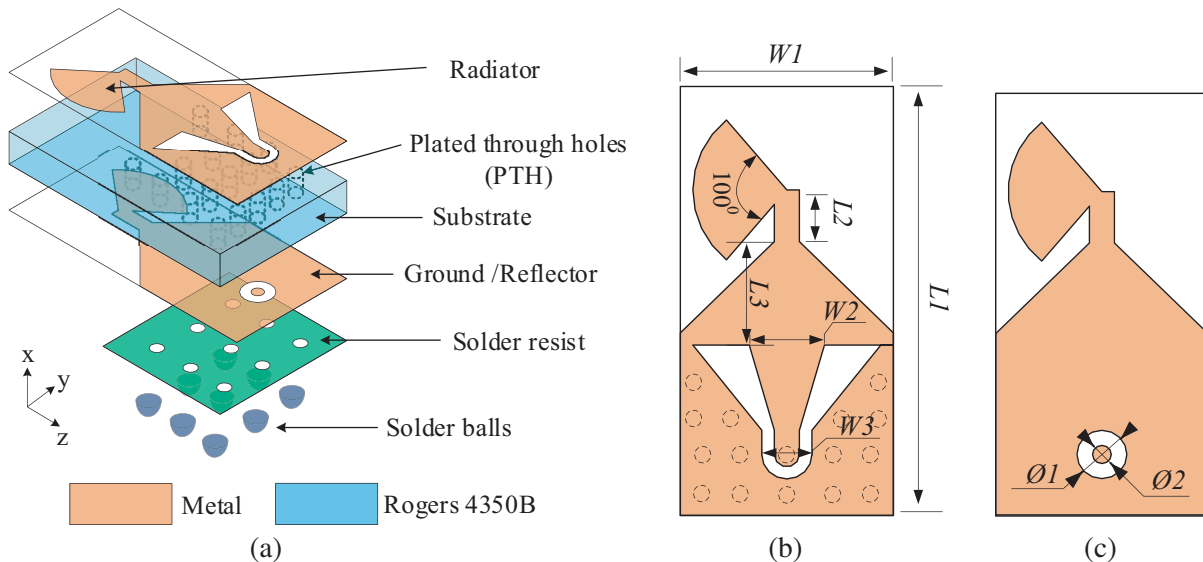
Figure 1. Geometry of the proposed antenna element. (a) Exploded view. (b) Top view. (c) Bottom view.

2.2. RF Transition

RF transition plays an important role in the transition of different transmission lines. The RF signal flows from the solder balls with an input impedance of 50 Ω to the bowtie patches through the PTH, grounded coplanar waveguide (GCPW), and SIW. There are two main RF transitions. One is from

Table 1. Dimensions of the proposed antenna element (Units: mm).

Parameters	Values	Parameters	Values
$L1$	7	$W2$	1.2
$L2$	0.85	$W3$	0.8
$L3$	1.51	$\Phi1$	0.8
$W1$	3.4	$\Phi2$	0.3

GCWP to SIW, and the other is vertical quasi-coaxial from solder ball to GCPW, which can be called BGA-via transition [22]. To better understand the RF transition, the E-field distribution of the antenna element at 38 GHz is shown in Figure 2. It can be seen that the transition from GCWP to SIW is formed by a tapered line to obtain better return loss. The PTH is the ideal E boundary around the tapered line, which reduces electromagnetic leakage. Similarly, a tapered line connects the SIW to the feedline to excite the bowtie patches. The BGA-via transition is a 50 Ω quasi-coaxial structure composed of solder balls and PTH to obtain a better reflection coefficient.
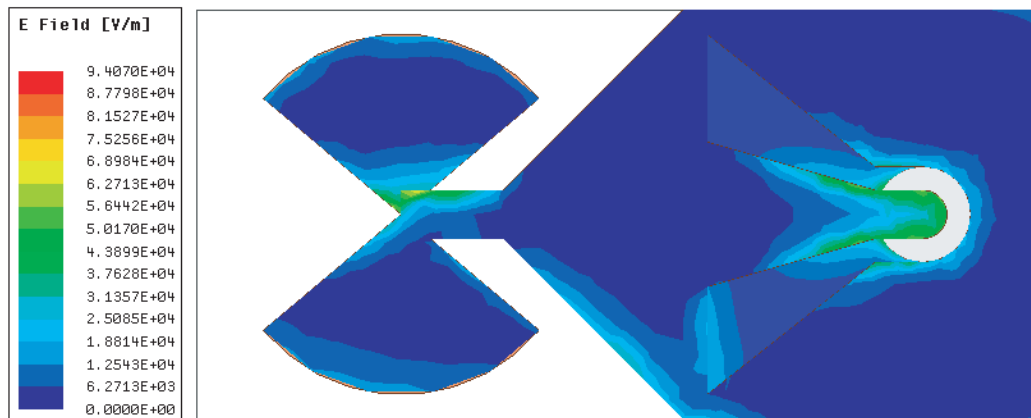
Figure 2. E-field distribution of the antenna element at 38 GHz.

2.3. Parametric Analysis

Manufacturing tolerances have a great influence on the performance of millimeter-wave antennas. To better understand the impact of tolerance on the reflection coefficient, the parameter analysis of $L2$ and $L3$ is shown in Figure 3. The scan value of $L2$ ranges from 0.75 to 0.95 mm, and the scan value of $L3$ ranges from 1.6 to 1.8 mm. Both scan steps are 0.1 mm. It can be seen that a larger $L2$ or $L3$ will expand the impedance bandwidth, and the reflection coefficient will also decrease at the center frequency. To balance the bandwidth and reflection coefficient, The final values of $L2$ and $L3$ are set to 0.85 mm and 1.7 mm, respectively.

3. MEASUREMENT RESULTS AND DISCUSSION

3.1. Measurement Condition

As depicted in Figure 4, a prototype is made to verify the design. The prototype is manufactured by using standard PCB processes. After the PCB processing is completed, solder balls are installed on the bottom layer of the prototype. Then the proposed antenna prototype is surface mounted on the Rogers4350B evaluation board with 50 Ω GCPW transmission lines. Besides, the size of the evaluation
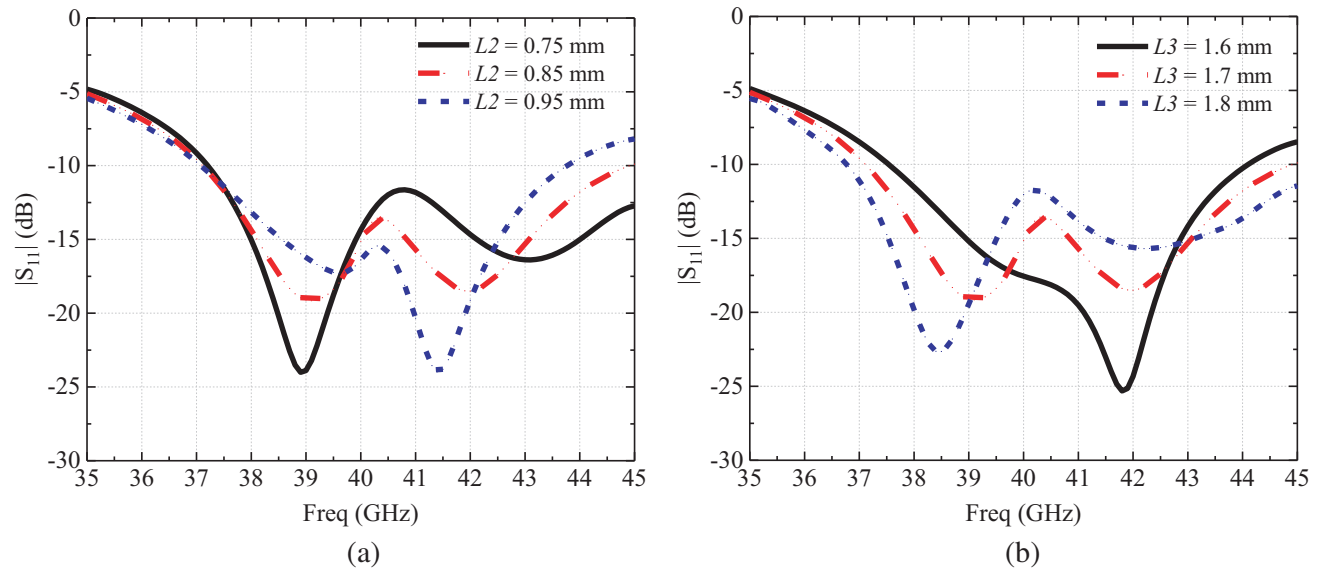
Figure 3. Parameter effects on reflection coefficient. (a) *L2*. (b) *L3*.
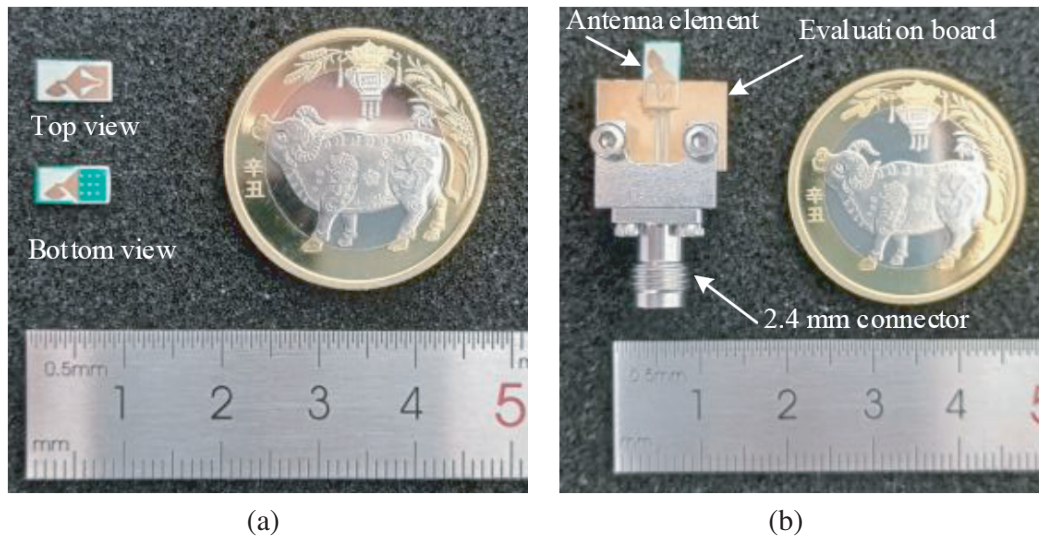
Figure 4. Photograph of the fabricated prototype. (a) Antenna element. (b) Assembled antenna element.

board is $14\,\text{mm} \times 13\,\text{mm} \times 0.254\,\text{mm}$. Finally, a 2.4 mm end launch connector (DC to 50 GHz) is installed at the end of the evaluation to connect the instrument's cable. The reflection coefficient is measured by the Keysight N5244A vector network analyzer (10 MHz to 43.5 GHz). The far-field radiation patterns are measured in an anechoic room with a standard horn antenna (26.5 to 40 GHz). Figure 5 shows the antenna under test (AUT) in the anechoic chamber.

3.2. Measured Results

The measured and simulated reflection coefficients are shown in Figure 6. The simulated $|S_{11}| < -10\,\text{dB}$ covers 37.1 to 44.6 GHz, while the measured $|S_{11}| < -10\,\text{dB}$ is 35.8 to 39.2 GHz and 41.7 to 43.5 GHz. Due to the limitation of our instrument, measurement data greater than 43.5 GHz are not given. The measured reflection coefficient varies from -9.9 to $-9.3\,\text{dB}$ in the range of 39.2 to 41.7 GHz. Figure 7
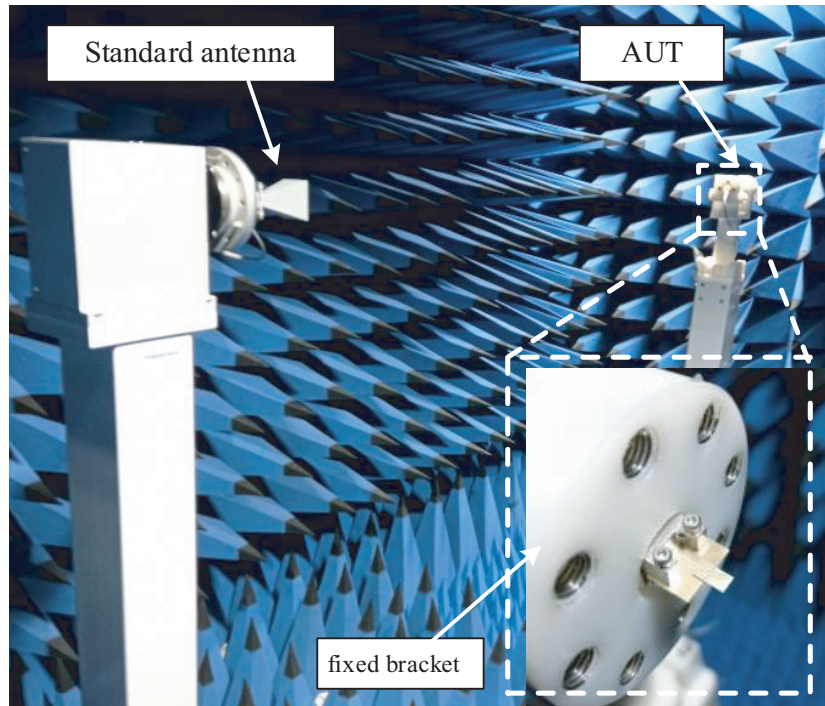
Figure 5. Photograph of the antenna under test in the anechoic chamber.
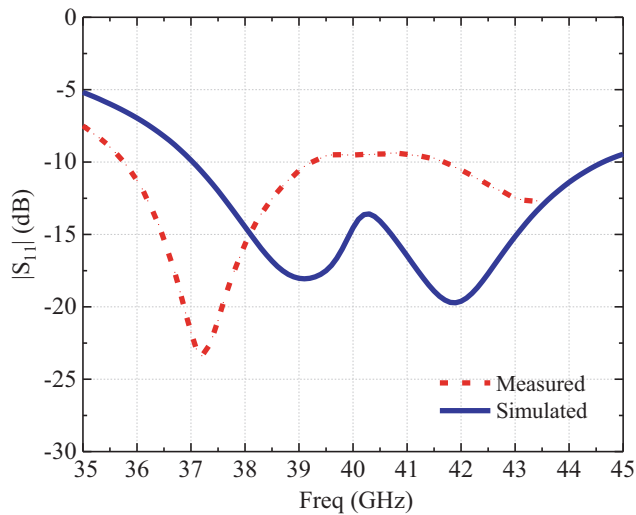
Figure 6. Measured and simulated $|S_{11}|$ of the prototype.
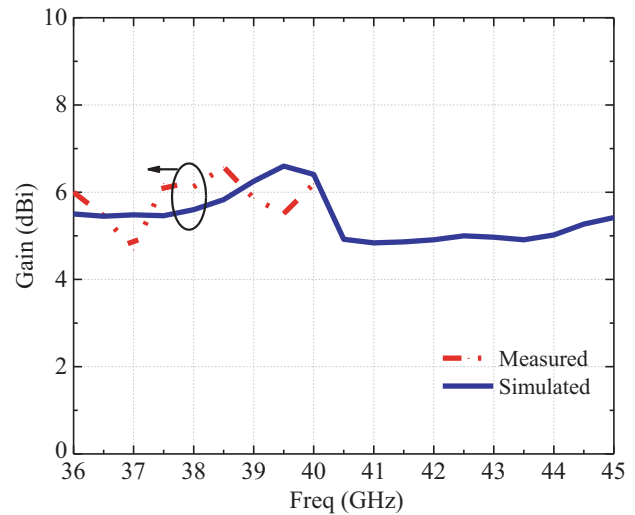
Figure 7. Measured and simulated gain and efficiency of the prototype.

depicts the measured and simulated gains of the prototype. The measured gain is between 4.67 and 6.85 dBi, and the simulated gain is between 5.45 and 6.6 dBi. Figure 8 shows the measured and simulated normalization radiation patterns of the antenna prototype at 37, 38, and 39 GHz, respectively.

It can be seen that there is a certain difference between the simulated data and measured results. From the above parametric analysis, the discrepancies between the simulated and measured results are mainly caused by the fabrication tolerance. Moreover, compared to the simulated radiation patterns, the measured radiation patterns are affected by the fixed bracket around the prototype.
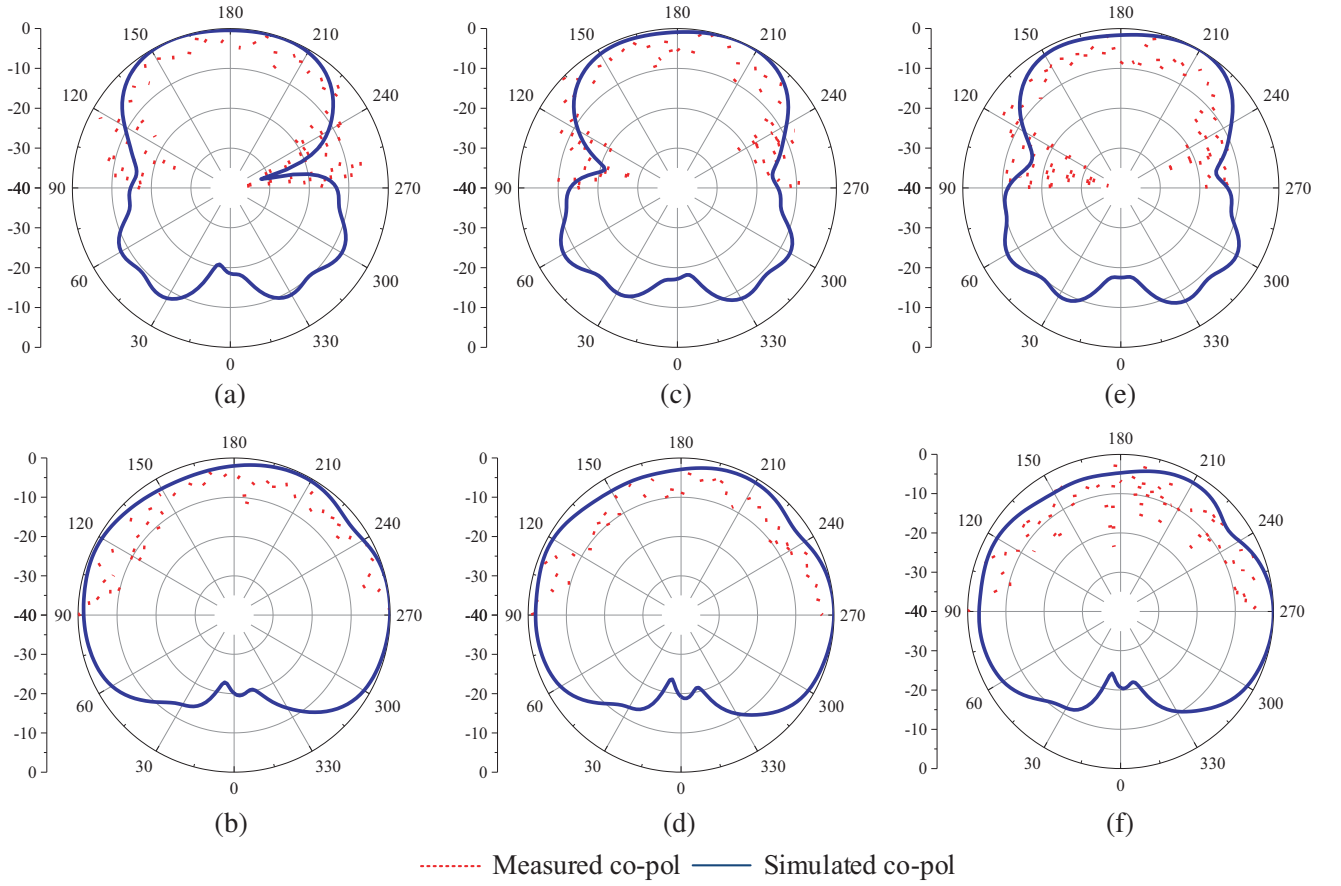
Figure 8. Measured and simulated normalization radiation patterns of the antenna prototype. (a) $f = 37$ GHz, E-plane. (b) $f = 37$ GHz, H-plane. (c) $f = 38$ GHz, E-plane. (d) $f = 38$ GHz, H-plane. (e) $f = 39$ GHz, E-plane. (f) $f = 39$ GHz, H-plane. (E-plane: YOZ; H-plane: XOZ).

Table 2. Comparisons between the proposed and reported antennas.

Ref.	Center Freq. (GHz)	Volume ($\lambda_0 \times \lambda_0 \times \lambda_0$)	Measured Imp. Bw (-10 dB)	Peak Gain (dBi)	Material	Number of dielectric layers	Cost
[3]	27.915	$0.22 \times 0.19 \times 0.11$	2.14%	4.54	Ro5880	4	Medium
[5]	27.9	$2.79 \times 1.85 \times 0.07$	8.6%	7.41	TLY-5	1	Low
[9]	26.87	$1.88 \times 0.87 \times 0.013$	19.53%	9.51	Glass	1	High
[12]	38.12	$0.69 \times 0.23 \times 0.11$	9.9%	2.43	LTCC	8	High
[16]	30.5	$0.6 \times 0.6 \times 0.27$	6.6%	7	-	14	High
[18]	5.715	$0.32 \times 0.32 \times 0.04$	4.1%	4.8	LTCC	3	High
[20]	60.65	$2.72 \times 1.62 \times 0.26$	14.3%	14.5	LTCC	4	High
This work	39.65	$0.93 \times 0.45 \times 0.08$	19.4%*	6.58	Ro4350B	1	Low

*-9.3 dB Measured impedance bandwidth

3.3. Comparison with Prior Works

As shown in Table 2, we compare some of the previously reported work with our proposed antenna. It can be seen that the reported antennas must be interconnected using coaxial connectors [3] or waveguide connectors [5], which is very difficult for system integration. In this work, BGA packaged antenna elements can be easily surface-mounted into the system package instead of using any bulky or lossy connectors. Compared with the multilayer configuration [12, 15, 16], the proposed antenna has the advantage of using a single-layer structure to reduce the cost. Besides, the higher gain and wider impedance bandwidth also make it become a good choice for the 5G mmWave system.

4. CONCLUSIONS

In this letter, the endfire antenna based on the BGA packaging has been successfully validated for the 5G mmWave system. The compact BGA package achieves a wide impedance bandwidth and a stable radiation pattern. Experimental results demonstrate that the proposed antenna can be used in the 5G mmWave NR frequency band (N259 39.5–43.5 GHz, N260 37–40 GHz). The features of compact size, low cost, easy integration, and compatibility with surface-mount technology make the proposed antenna more attractive for 5G mmWave NR systems.

ACKNOWLEDGMENT

REFERENCES

1. Andrews, J. G., et al., "What will 5G be?," *IEEE J. Sel. Areas Commun.*, Vol. 32, No. 6, 1065–1082, Jun. 2014.
2. Rappaport, T. S., et al., "Millimeter wave mobile communications for 5G cellular: It will work!," *IEEE Access*, Vol. 1, 335–349, 2013.
3. Tang, M., T. Shi, and R. W. Ziolkowski, "A study of 28 GHz, planar, multilayered, electrically small, broadside radiating, huygens source antennas," *IEEE Trans. Antennas Propag.*, Vol. 65, No. 12, 6345–6354, Dec. 2017.
4. Lin, W., R. W. Ziolkowski, and T. C. Baum, "28 GHz compact omnidirectional circularly polarized antenna for device-to-device communications in the future 5G systems," *IEEE Trans. Antennas Propag.*, Vol. 65, No. 12, 6904–6914, Dec. 2017.
5. Park, J., J. Ko, H. Kwon, B. Kang, B. Park, and D. Kim, "A tilted combined beam antenna for 5G communications using a 28-GHz band," *IEEE Antennas Wirel. Propag. Lett.*, Vol. 15, 1685–1688, 2016.
6. Zhang, Y., "Antenna-in-package technology: Its early development [historical corner]," *IEEE Antennas Propag. Mag.*, Vol. 61, No. 3, 111–118, Jun. 2019.
7. Zhang, Y. and J. Mao, "An overview of the development of antenna-in-package technology for highly integrated wireless devices," *Proc. IEEE*, Vol. 107, No. 11, 2265–2280, Nov. 2019.
8. Watanabe, A. O., M. Ali, S. Y. B. Sayeed, R. R. Tummala, and M. R. Pulugurtha, "A review of 5G front-end systems package integration," *IEEE Trans. Compon. Packag. Manuf. Technol.*, Vol. 11, No. 1, 118–133, Jan. 2021.
9. Ali, M., et al., "Package-integrated, wideband power dividing networks and antenna arrays for 28-GHz 5G new radio bands," *IEEE Trans. Compon. Packag. Manuf. Technol.*, Vol. 10, No. 9, 1515–1523, Sep. 2020.
10. Jin, C., V. N. Sekhar, X. Bao, B. Chen, B. Zheng, and R. Li, "Antenna-in-package design based on wafer-level packaging with through silicon via technology," *IEEE Trans. Compon. Packag. Manuf. Technol.*, Vol. 3, No. 9, 1498–1505, Sep. 2013.

11. Choi, J., D. Choi, J. Lee, W. Hwang, and W. Hong, "Adaptive 5G architecture for an mmWave antenna front-end package consisting of tunable matching network and surface-mount technology," *IEEE Trans. Compon. Packag. Manuf. Technol.*, Vol. 10, No. 12, 2037–2046, Dec. 2020.

12. Park, J., H. Seong, Y. N. Whang, and W. Hong, "Energy-efficient 5G phased arrays incorporating vertically polarized endfire planar folded slot antenna for mmWave mobile terminals," *IEEE Trans. Antennas Propag.*, Vol. 68, No. 1, 230–241, Jan. 2020.

13. Beer, S., H. Gulan, C. Rusch, and T. Zwick, "Coplanar 122-GHz antenna array with air cavity reflector for integration in plastic packages," *IEEE Antennas Wirel. Propag. Lett.*, Vol. 11, 160–163, 2012.

14. Beer, S., et al., "An integrated 122-GHz antenna array with wire bond compensation for SMT radar sensors," *IEEE Trans. Antennas Propag.*, Vol. 61, No. 12, 5976–5983, Dec. 2013.

15. Liu, D., X. Gu, C. W. Baks, and A. Valdes-Garcia, "Antenna-in-package design considerations for Ka-band 5G communication applications," *IEEE Trans. Antennas Propag.*, Vol. 65, No. 12, 6372–6379, Dec. 2017.

16. Gu, X., et al., "Development, implementation, and characterization of a 64-element dual-polarized phased-array antenna module for 28-GHz high-speed data communications," *IEEE Trans. Microw. Theory Tech.*, Vol. 67, No. 7, 2975–2984, Jul. 2019.

17. Tsai, C. H., et al., "Fabrication and characterization of millimeter wave 3D InFO dipole antenna array integrated with CMOS front-end circuits," *2019 IEEE International Electron Devices Meeting (IEDM)*, 25.3.1–25.3.4, Dec. 2019.

18. Zhang, Y. P., "Integration of microstrip patch antenna on ceramic ball grid array package," *Electron. Lett.*, Vol. 38, No. 5, 207–208, Feb. 2002.

19. Zhang, Y. P., "Integrated circuit ceramic ball grid array package antenna," *IEEE Trans. Antennas Propag.*, Vol. 52, No. 10, 2538–2544, Oct. 2004.

20. Sun, M., Y. P. Zhang, D. Liu, K. M. Chua, and L. L. Wai, "A ball grid array package with a microstrip grid array antenna for a single-chip 60-GHz receiver," *IEEE Trans. Antennas Propag.*, Vol. 59, No. 6, 2134–2140, Jun. 2011.

21. Tong, Z., A. Fischer, A. Stelzer, and L. Maurer, "Radiation performance enhancement of E-band antenna in package," *IEEE Trans. Compon. Packag. Manuf. Technol.*, Vol. 3, No. 11, 1953–1959, Nov. 2013.

22. Kangasvieri, T., J. Halme, J. Vahakangas, and M. Lahti, "Broadband BGA-via transitions for reliable RF/microwave LTCC-SiP module packaging," *IEEE Microw. Wirel. Compon. Lett.*, Vol. 18, No. 1, 34–36, Jan. 2008.